

Indoor Position Detection Using BLE Signals Based on Voronoi Diagram

Kensuke Onishi^(✉)

Tokai University, 4-1-1 Kitakaname, Hiratsuka, Kanagawa 259-1292, Japan
onishi@tokai-u.jp

Abstract. Bluetooth Low Energy (BLE) is a Bluetooth standard with low energy consumption. Beacons using BLE transmit BLE signals, which can be received by smart phones running iOS or Android OS. At present, demonstration experiments are conducted.

An indoor position detection using an ordered order- k Voronoi diagram was proposed. Beacons were installed in a building of Tokai University. Experiments are conducted to investigate position detection using the proposed approach. We have two results using the proposed system: (1) a floor decision success rate of 99.6 %; and (2) indoor position detection success rates of 85.5 % (first neighbor) and 48.9 % (second neighbor). Finally, we present some ideas for improving the proposed approach.

1 Introduction

Bluetooth Low Energy (BLE) [1] is a low-power Bluetooth standard. A machine called a *beacon* is developed for use in transmitting BLE signals. The beacon works for approximately one year on only a button battery.

BLE has been supported by iOS since 2013 and by Android OS (after version 4.3) since 2014. A BLE signal can be received by numerous types of smart phone. Thus, a number of demonstration experiments have been conducted in various locations. For example, beacons were placed on each aquarium at Hakkeijima Sea Paradise. When a person approaches one of the aquarium with a smart phone, the smart phone displays information on the sea animals in the aquarium ([2], until March 2015). A number of beacons have been placed in Tokyo Station to support position detection and navigation ([3], until February 2015). Finally, a system was constructed in which information related to bus stops was provided by beacons placed in busses in Kyoto City [4].

A number of studies have examined position detection based on a received signal: GPS (outdoors) and WiFi [5–7] (indoors). In a previous study, the Received Signal Strength Indicator (RSSI) of a WiFi access point was measured at many points, and a method of position detection using the measured data was proposed [5]. The covering method of directional sensor networks using Voronoi diagram was proposed [8]. While the directional sensor distributes signals for a pie-shaped region, the beacon distributes for all range. Moreover, an experiment using BLE signals had been conducted [9], in which 50 beacons were placed in a real field and the RSSIs of the BLE signals were measured. The position decision

by BLE signal was performed with an accuracy of 10 m to 20 m, and a hybrid method using the BLE signal and pedestrian dead reckoning was proposed.

We consider the problem for detecting own position from given field and installed beacons. It is necessary that the BLE signals from beacons cover the field. When many beacons are installed, the problem can be solved easily. BLE signals are collected by user's smart phone, then it is decided that the user is near the beacon with strongest RSSI. It has expensive cost that many beacons install on a real field. We consider indoor position detection under small number of beacons where the BLE signals cover the field.

In the present paper, we propose a method for position detection based on an ordered order- k Voronoi diagram. The Voronoi diagram is easily computed at a desk, and a number of configurations of beacons can be planned. We decided a configuration of beacons for a building of Tokai University, then installed 30 beacons on the building and measured the RSSIs of the BLE signal. We then evaluate the proposed method based on the measurement data. We explain the ordered order- k Voronoi diagram in Sect. 2, and the proposed method is described in Sect. 3. In Sect. 4, we describe the beacons used in the experiments, the building in which the experiments are conducted, and the experiments themselves. The experiments are further discussed floor decision and indoor position detection in Sect. 5.

2 Related Research

2.1 Ordered Order- k Voronoi Diagram

In this section, we explain the ordered order- k Voronoi diagram. Consider a set of points $P = \{p_1, p_2, \dots, p_n\}$. Each point in the set is called a *site*. Let $(p_{i_1}, p_{i_2}, \dots, p_{i_k})$ be ordered sites selected from P . An ordered order- k Voronoi diagram [10, pp. 144–151], called an *OO- k Voronoi diagram*, is a tessellation and consists of ordered order- k Voronoi polygons $R(P; i_1, i_2, \dots, i_k)$. The ordered order- k Voronoi polygon is defined as follows:

$$\begin{aligned} R(P; i_1, i_2, \dots, i_k) \\ = \{x \in \mathbf{R}^2 \mid d(x, p_{i_1}) < d(x, p_{i_2}) < \dots < d(x, p_{i_k}) < d(x, p_j), \\ j \neq i_1, i_2, \dots, i_k\}, \end{aligned}$$

where $d(x, y)$ is the Euclidean distance between x and y . This polygon is a convex subset of the Euclidean plane. Every point in the polygon is near $p_{i_1}, p_{i_2}, \dots, p_{i_k}$ in the order. The set of Voronoi polygons for all ordered k sites is referred to as an OO- k Voronoi diagram.

Figure 1 is an OO-3 Voronoi diagram for P , which has six sites. The solid lines in Fig. 1 form the (OO-1) Voronoi diagram for the point set, which gives the nearest region of each site. The solid and dashed lines form the OO-2 Voronoi diagram. Each OO- k Voronoi polygon is divided into a number of OO- $(k + 1)$ Voronoi polygons. In Fig. 1, $R(P; 4, 3)$ is divided into $R(P; 4, 3, 2)$, $R(P; 4, 3, 5)$, and $R(P; 4, 3, 6)$.

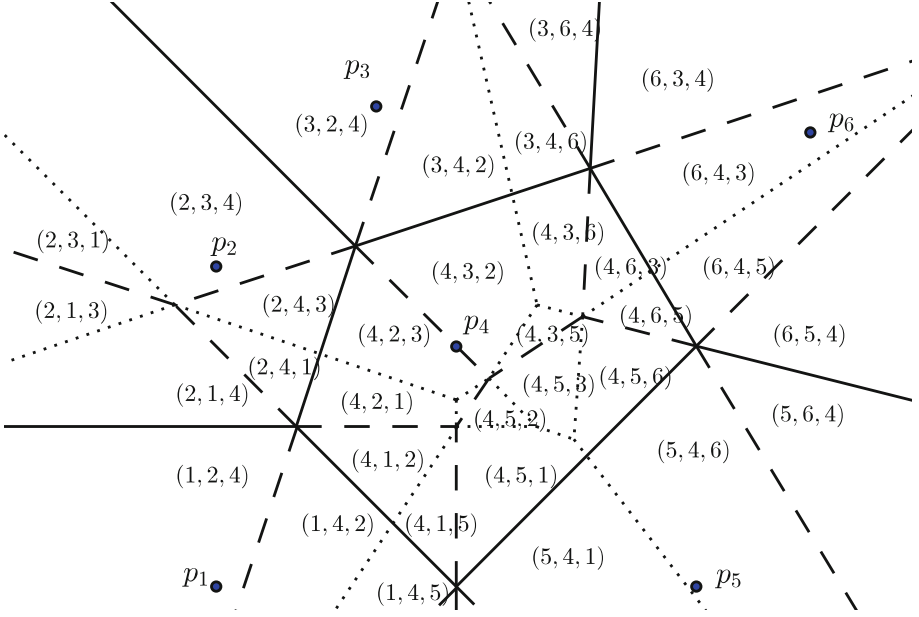


Fig. 1. Ordered order-3 Voronoi diagram.

The OO- k Voronoi diagram is constructed in $O(nk^2 \log n + nk \log^3 n)$ time and $O(k(n - k))$ storage [11]. Lee et al. proposed a computation method of generalized higher-order Voronoi diagram (HOVD) and applied HOVD to map segmentation [12].

2.2 Arrangement

The arrangement is formed by lines in a Euclidean plane. Consider n lines in the plane. The plane is divided into regions consisting of segments formed by given lines. The arrangement of n lines is computed in $O(n^2)$ time and $O(n^2)$ space [13]. The OO- n Voronoi diagram for n sites has the same structure with an arrangement of perpendicular bisectors of all pair of sites.

3 Proposed Method

In this section, we describe the proposed algorithm for position detection. The proposed algorithm uses position detection by an ordered order- k Voronoi diagram, or an arrangement of perpendicular bisections of all pair of sites.

Suppose that the configuration of beacons is known. We compute the OO- k Voronoi diagram, or the arrangement of beacon sites. Each OO- k polygon is regarded as position in indoor position detection. So we evaluate the difference among the OO- k polygon and the ordered sequence of beacons sorted by RSSI on a real field. Then, we clarify the problems of proposed method.

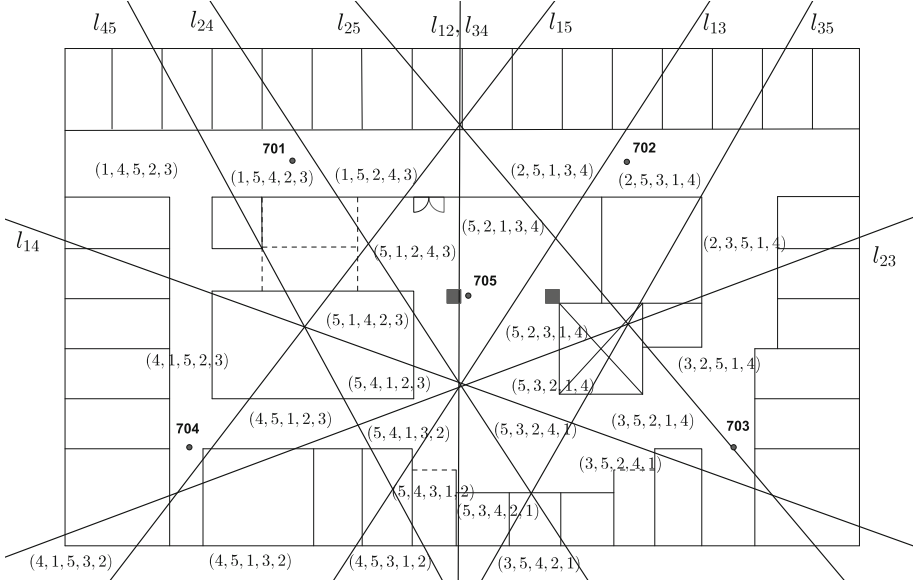


Fig. 2. Ordered order-5 Voronoi diagram on the seventh floor of Building 18 at Tokai University.

Figure 2 shows an OO-5 Voronoi diagram of the seventh floor of Building 18 at Tokai University. We installed five beacons (701–705) on the seventh floor, and five beacons were placed on the other floors. The configuration of beacons was planned to cover the field by small number of beacons. The seventh floor was divided into a number of OO-5 Voronoi polygons.

When position detection is performed using BLE signals, a smart phone collects signals from the beacons. The beacons are then sorted by RSSI and the beacon order is used to determine current position. For example, suppose that the sorted sequence of beacons is 704, 705, 701, 804, 702, 604, 703, 601, 801, as shown in Fig. 2. Suppose that we already know that we are on the seventh floor. Since beacons 6** and 8** are on the sixth and eighth floors, respectively, we use only the 7** beacons: 704, 705, 701, 702, 703. Then our position on the seventh floor is decided as $R(\bar{P}; 4, 5, 1, 2, 3)$.

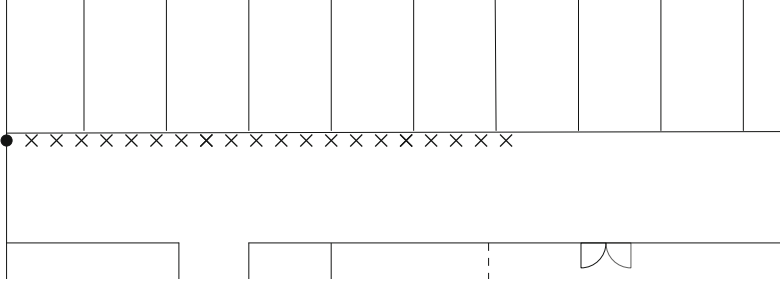
The floor can be also decided based on the sorted sequence of beacons from the frequencies of first digits. If two first-digit values have the same number of occurrences, then we select the value corresponding to stronger BLE signals. In the above example, the first digits are (7, 7, 7, 8, 7, 6, 7, 6, 8). Since 6, 7 and 8 appear once, five times and two times, respectively, in the sequence, the floor is decided as the seventh.

Table 1. Specifications of the beacons.

Model Name	HRM1017
Embedded BLE chip	Nordic nRF51822
Bluetooth version	Bluetooth LE 4.0 (Single mode)
QDID	B020660
RF output power	−8 dBm type
Supply voltage	1.8 to 3.6 V

Table 2. Specifications of Nexus 7 (2013, WiFi).

Model Name	Nexus 7 (2013, WiFi)
Manufacturer	ASUS
OS	Android 5.0.2 (Lollipop)
CPU	APQ8064(1.5 GHz)
Main Memory	2 GB
Storage	16 GB

**Fig. 3.** Measurement points at the upper left corner of the seventh floor. ●: beacon, ×: measurement point.

4 Measurement of the Beacon Field

4.1 Beacons and Smart Phone

First, we explain the beacon (Houwa System Design K.K.) and the smart phone used in the present study. The BLE module in the beacon is an HRM1017 (Hosiden Corp.). The supply voltage is approximately 3.0 V. The beacon can change the output power from −20 dBm to +4 dBm. Since the floor area is 32.8m by 52.8m and keeping the power as low as possible, we use −8 dBm in our experiment. The specifications of the beacons are shown in Table 1.

We use the Nexus 7 (2013, WiFi) as the BLE signal receiver. The Nexus 7 runs on Android 5.0.2 and supports a BLE device. The specifications of the receiver are shown in Table 2.

4.2 Preliminary Experiment

In this section, we describe the basic performance of beacons in a real location. We place one beacon in the upper left corner of the seventh floor. We measured the RSSI from 1 to 20m at intervals of 1 m (Fig. 3). On average 46.5 measurements were taken at each measurement point, where a measurement consisted of sensing in four directions, each requiring 10 s. Measurements were then averaged over the four directions in order to account for local variation in a real location.

Figure 4 shows a box-and-whisker plot of the measurements. The x axis indicates the distance from the beacon and the y axis indicates the dBm level.

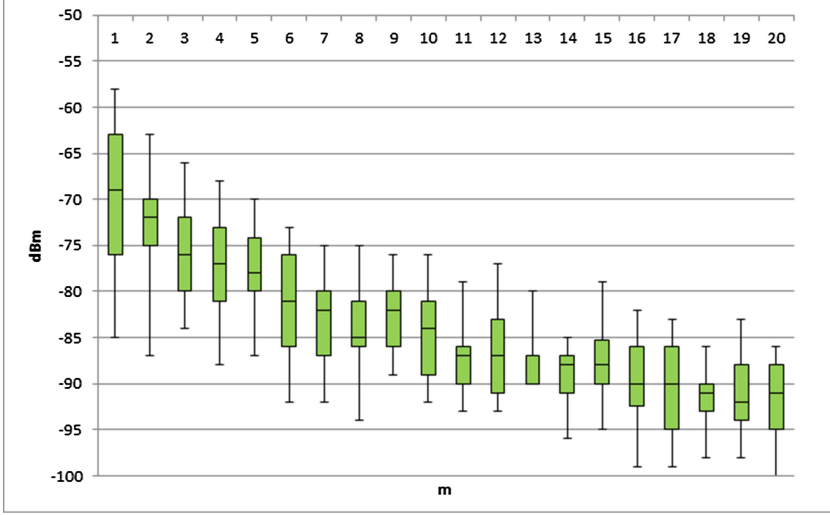


Fig. 4. Measurement results: RSSI (dBm) vs. distance (m)

In general, RSSI decreased with increasing distance, although there was some variation.

In this situation, we can find two thresholds: -65 dBm and -80 dBm. When the RSSI is larger than -65 dBm, the smart phone is closest to the beacon (corresponding to *Immediate* in the iOS SDK [14]). When the RSSI is larger than -80 dBm, the smart phone is near the beacon (corresponding to *Near* in the iOS SDK). Thus, we can divide the distance from the beacon into four parts: *Immediate* (RSSI > -65 dBm), *Near* (-80 dBm $<$ RSSI < -65 dBm), *Far*¹ (RSSI < -80 dBm) and *Unknown* (BLE is not detected).

4.3 Experiment on the Beacon Field

In this section, we describe the arrangement of beacons on the seventh floor of Building 18 at Tokai University. The arrangement of beacons is referred to as the *beacon field* and, in the following, we describe the measurement results on the beacon field.

Figure 5 shows the measurement points in the beacon field. The beacons are indicated by \bullet symbols and measurement points are indicated by \times symbols. We measured 136 points in the field. At each point, we measured in four directions, each requiring approximately 10 s. The average number of measurements is 41.7 per measurement point. The average number of measured beacons used in a measurement is 8.47.

¹ *Immediate*, *Near*, *Far* and *Unknown* are the return values for a method in the iOS SDK.

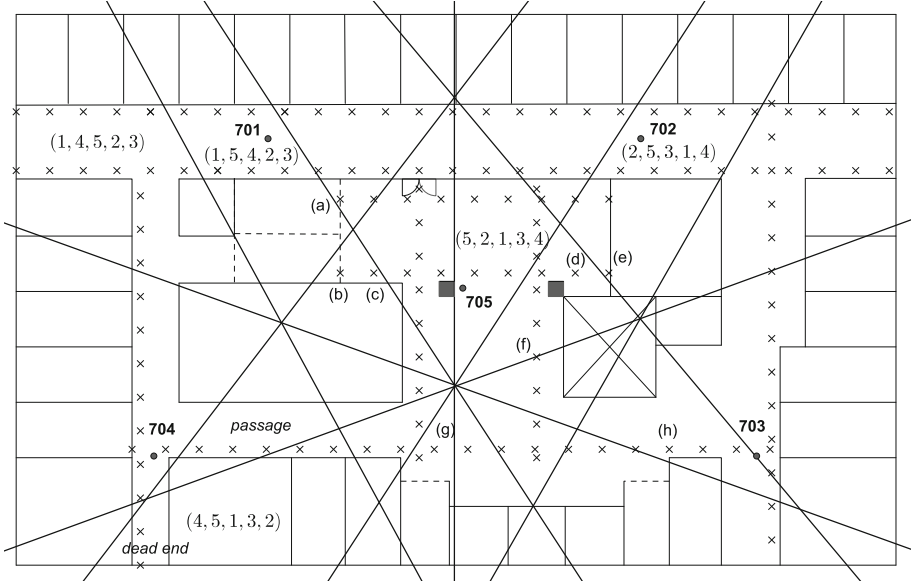


Fig. 5. Measurement points (\times) and ordered order-5 Voronoi diagram for beacons (\bullet) on the seventh floor.

Table 3. Floor decision rate statistics.

Measurement point	All	(a)	(b)	(c)	(d)	(e)	(f)	(g)	(h)
Correct rate	0.9961	0.8684	0.8837	0.8974	0.8205	1.0000	1.0000	1.0000	0.9767
Mistake rate	0.0039	0.1316	0.1163	0.1026	0.1795	0.0000	0.0000	0.0000	0.0233
Same rate	0.0580	0.4211	0.3023	0.5385	0.3333	0.3721	0.4524	0.4048	0.2093

Table 3 lists the correct and mistake rates for all and the measurement points (a), (b), \dots , (h) shown in Fig. 5. The table also lists the *same rate*, which is the rate that two first-digit values have the same number of occurrences.

Table 4 lists the *correct rates* of OO- k Voronoi polygons in the experiments. The correct rate is computed as follows. Each measurement point is contained in an OO-5 Voronoi polygon. Thus, every point has a correctly sorted sequence of beacons $(c_1, c_2, c_3, c_4, c_5)$. In a measurement, we have a measured sequence of beacons (b_1, b_2, \dots, b_k) . The number k of measured beacons is not always five, but the maximum number of measured beacons is five. If b_j is equal to c_j ($j = 1, \dots, i$), we decide that these b_j are correctly ordered. When b_{i+1} is not equal to c_{i+1} , the beacons b_{i+1}, \dots, b_k are counted as an incorrect answer if $b_k = c_k$. As the index i increases, the correct rate decreases. The correct rate r_i of a OO- i Voronoi polygon is the number of correct beacons divided by the number of i th measurement beacons.

Table 4. Correct rates of ordered order- k Voronoi polygons.

Region	First	Second	Third	Fourth	Fifth	Number of measurement points
average	0.854648086	0.489470890	0.285739910	0.160785054	0.076366359	136
14523	0.840579710	0.378870674	0.113382900	0.075848303	0.000000000	14
15243	0.809224319	0.360379347	0.198505870	0.087640449	0.002074689	10
15423	0.848962656	0.309166667	0.156565657	0.068904594	0.001533742	6
23514	0.879654614	0.352685838	0.180011044	0.120669056	0.064893617	15
25134	0.841876629	0.353839442	0.211061947	0.132672332	0.074738416	11
25314	0.857825129	0.381180812	0.202616822	0.135124457	0.070960048	10
32514	0.870627063	0.386808088	0.223759703	0.135416667	0.066773504	7
35241	0.871857013	0.409671533	0.238995660	0.142051112	0.063383715	6
41523	0.882191781	0.448693260	0.262111453	0.138688327	0.064183124	9
45123	0.886483633	0.457195865	0.27015368	0.142237641	0.068365180	3
45132	0.89107413	0.470260693	0.284684685	0.152509653	0.074918567	4
51243	0.870967742	0.473364801	0.298333714	0.168042739	0.079146593	12
51423	0.865112225	0.468299082	0.290279627	0.163169064	0.076411960	3
52134	0.858987497	0.472245066	0.301878914	0.173893805	0.084502746	7
52314	0.857312959	0.482085987	0.303152789	0.174080411	0.083625731	4
53214	0.859652547	0.476311668	0.299284579	0.171848739	0.081621005	2
53241	0.857302326	0.488337376	0.293961764	0.168696347	0.080610605	6
53421	0.858171745	0.486015929	0.292692091	0.168350168	0.081102571	1
54123	0.857011916	0.484096341	0.290509043	0.167026921	0.080293886	1
54132	0.855686695	0.489418938	0.286000000	0.163030999	0.077743902	3
54312	0.854648086	0.489470890	0.285739910	0.160785054	0.076366359	2

For example, a measurement point is contained in $R(P; 1, 5, 2, 4, 3)$. We measured a sorted sequence of beacons (*701, 801, 704, 805, 702, 602, 505, 703, 804, 705, 502, 803*) on the seventh floor. We only use γ^{**} : (*701, 704, 702, 703, 705*). We judge the first beacon *701* to be correct and the other beacons to be incorrect.

Figure 6 is a graph of the correct rates of average regions, good regions $R(P; 4, 5, 1, 3, 2)$, $R(P; 5, 2, 1, 3, 4)$ and worse regions $R(P; 1, 5, 4, 2, 3)$, $R(P; 1, 4, 5, 2, 3)$.

5 Discussion

Floor Decision

The floor decision is successful for 5,652 out of 5,674 measurements. The mistake rate is only 3.9% in Table 3. The measurement points from (a) to (h) in Fig. 5 and in Table 3 includes ones with mistake decisions, or same rates higher rather than 40%. We divide these points into three groups: $\{(a), (b), (c)\}$, $\{(d), (e), (f)\}$, and $\{(g), (h)\}$. The first group $\{(a), (b), (c)\}$ is near staircases. The area indicated by the dashed lines containing (a) and (b) in Fig. 5 is the foot of the staircases. Since the staircases connect to the sixth and eighth floors, the smart phone collects BLE signals from other floors. This is why incorrect floor decisions

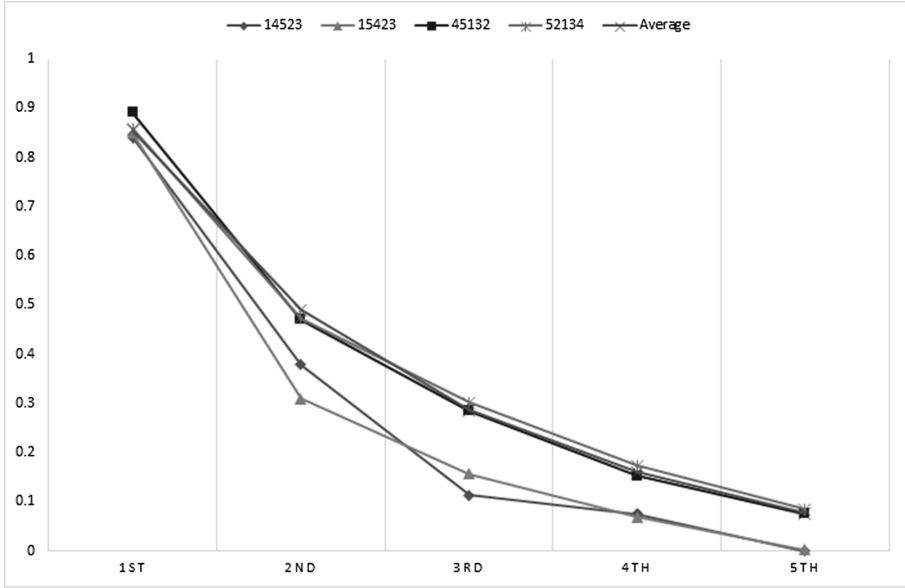


Fig. 6. Correct rates of some Voronoi polygons.

are made. Each of the third group $\{(g), (h)\}$ is also near the foot of staircases, again indicated by dashed lines.

The second group $\{(d), (e), (f)\}$ is not near staircases, but rather the measurement points are near a glass-enclosed open ceiling space, as expressed by \boxtimes in Fig. 5. The BLE signal from the upper floor comes in through the glass.

Position Detection

[Average Rate]. First, we discuss the average correct rate of OO- k Voronoi polygons in Table 4. The first and second neighbors have correct rates of 85.5 % and 48.9 %, respectively. The remaining neighbors are 28.6 %, 16.0 %, and 7.6 %, in sequence. The first and second neighbors can be used for position detection, whereas the other neighbors cannot.

[Good Correct Rates]. In this section, we focus on polygons $R(P; 4, 5, 1, 3, 2)$ and $R(P; 5, 2, 1, 3, 4)$. Polygon $R(P; 4, 5, 1, 3, 2)$ is the lower left region in Fig. 5 and contains five measurement points. The measurement points are divided into two regions: the *dead end* and the *passage*. While the BLE signals from beacons 704 and 705 are received in the passage, the signal from beacon 704 is received in the dead end. Although the measurement point in the dead end is near beacon 705, the RSSI of beacon 705 is smaller than that of beacon 701, since there are walls between beacon 705 and the measurement points. Thus, the correct ratio of the points in the passage is better than that of the points in the dead end.

Polygon $R(P; 5, 2, 1, 3, 4)$ is the middle region in Fig. 5. There are seven measurement points in $R(P; 5, 2, 1, 3, 4)$, six of which are near beacon 705 and one of which is on the other side of a glass wall. At the point on the other side of glass, the RSSIs of beacons 701 and 702 are larger than that of beacon 705. Thus, the correct rate is lower at the point and the average correct rate of $R(P; 5, 2, 1, 3, 4)$ is also lower. For better indoor position detection, it is necessary to omit such a point from the polygon, or to take the attenuation by the glass wall into consideration.

[Poor Correct Rates]. We discuss OO-5 Voronoi polygons $R(P; 1, 5, 4, 2, 3)$ and $R(P; 1, 4, 5, 2, 3)$. The polygon $R(P; 1, 5, 4, 2, 3)$ is located in the upper left corner of the beacon field (see Fig. 5). Among the measurement points of polygon $R(P; 1, 5, 4, 2, 3)$, the RSSIs of beacons 702 and 704 are larger than those of beacon 705. The reason for this is that a glass wall and a staircase exist between the polygon and beacon 705. The RSSI of 705 is weakened by the wall and by the large interference from beacons on other floors. The situation of polygon $R(P; 2, 5, 3, 1, 4)$ is similar to that of polygon $R(P; 1, 5, 4, 2, 3)$ from the symmetry of the configuration of beacons. The differences of situation between these polygons is near the staircases, or not. While beacon 705 is found 38 % measurement in polygon $R(P; 2, 5, 3, 1, 4)$, 705 is 30 % in polygon $R(P; 1, 5, 4, 2, 3)$. It is consider that the difference of correct rate is interference from other floors.

The polygon $R(P; 1, 4, 5, 2, 3)$ is also located in the upper left corner of the beacon field. The correct rates are 84 %, 38 %, 11 %, 8 % and 0 %, in sequence. Whereas the first rate is about the same as the average, the remaining rates are below the average. Thus, beacons 702 and 704 are detected and beacon 705 is not detected. The reason for this is also the above-mentioned interference.

6 Conclusion

In the present paper, we propose a method for indoor position detection using an ordered order- k Voronoi diagram. The proposed method involves two steps: floor decision and position detection. In the floor step, the floor number is decided based on the measured RSSIs. Position detection is based on a sequence of beacons arranged in strength order. The beacon field is divided into OO- k Voronoi polygons for sites that correspond to beacons.

We installed beacons in Building 18 of Tokai University and measured RSSIs at several points on seventh floor. We evaluated the measurements based on *floor decision* and *position detection*.

The floor decision success rate was approximately 99.6 %. At a few measurement points, the decision fails because of BLE signals from other floors. One idea is that used beacon is limited by their RSSIs (> -65 dBm) for detail decision. Since the beacons at other floor are far from a measurement point in a floor, the BLE signals from the beacons are weak. By the limitation, such beacons can be pruned from the sequence of beacons.

The position detection success rates are 85.5 % (first neighbor), 48.9 % (second neighbor) and 28.6 % (third neighbor). The first and second neighbors can be used for position detection. Two problem for position detection are found. One is interference of signals, another is variations of wall. First problem is a reason of worse correct ratio in higher order. The essential solution is difficult. We only take measure by the adjustment of neighbor region on real field. Another problem is solved by considering transmittance of wall. The glass wall above partially transmits BLE signals whereas the concrete wall does not transmit at all. So, we consider transmittance of wall and apply to proposed method.

For the effective use of these neighbors, it is better to use an *order- k Voronoi diagram*. A polygon $R(P; \{i_1, \dots, i_k\})$ of an order- k Voronoi diagram is constructed by combining all OO- k Voronoi polygons $R(P; \sigma(i_1), \dots, \sigma(i_k))$, where σ is a permutation of i_1, i_2, \dots, i_k . For example, $R(P; \{2, 4\})$ in Fig. 1 is the combination of $R(P; 2, 4)$ and $R(P; 4, 2)$. Since the number of order- k Voronoi polygons is less than the number of OO- k polygons, we place more beacons on the field. HOVD [12] is also useful for indoor position detection when all wall does not transmit BLE signals.

The adjacency of an OO- k Voronoi polygon is useful for better detection. When a person is in an OO- k Voronoi polygon, in general, the person can only move to adjacent polygons.² For example, $R(P; 2, 4, 3)$ is adjacent to only $R(P; 2, 3, 4)$, $R(P; 4, 2, 3)$ and $R(P; 2, 4, 1)$.

Acknowledgments. The author would like to thank Professor Yoshimi ISHIHARA, Dean of the School of Science, Tokai University, for allowing the installation of beacons on Building 18 and for providing the opportunity to conduct the present study. Thanks are also due to Professor Masanori ITAI for suggesting the beacon installation and to the Open Beacon Field Trial (OBFT) (<http://openbeacon.android-group.jp/>) for providing beacons as well as the opportunity to conduct the present study. Special thanks are due to Daiki KANAI, a student in my laboratory, for measuring the RSSIs of the beacons.

References

1. Bluetooth specifications version 4.0, June 2010. <https://www.bluetooth.org/>
2. Yokohama Hakkeijima Sea paradise. <http://www.seaparadise.co.jp/english/>
3. Tokyo station navigation, East Japan Railway Company. <http://www.jreast.co.jp/e/>
4. Kyoto City Bus. <http://www2.city.kyoto.lg.jp/koho/eng/access/transport.html>
5. Hatami, A., Pahlavan, K.: A Comparative performance evaluation of RSS-based positioning algorithms used in WLAN networks. In: Proceedings of the IEEE Wireless Communications and Networking Conference (WCNC 2005), vol. 4, pp. 2331–2337, New Orleans, USA, March 2005
6. Evennou, F., Marx, F.: Advanced integration of WiFi and inertial navigation systems for indoor mobile positioning. EURASIP J. Appl. Signal Process 2006, Article ID 86706, 1–11 (2006). doi:[10.1155/ASP/2006/86706](https://doi.org/10.1155/ASP/2006/86706)

² Two Voronoi polygons are adjacent when the polygons share a segment.

7. Lloret, J., Tomas, J., Garcia, M., Canovas, A.: A hybrid stochastic approach for self-location of wireless sensors in indoor environments. *Sensors* **9**, 3695–3712 (2009). doi:[10.3390/s90503695](https://doi.org/10.3390/s90503695)
8. Sung, T.-W., Yang, C.-S.: Voronoi-based coverage improvement approach for wireless directional sensor networks. *J. Netw. Comput. Appl.* **39**, 202–213 (2014)
9. Ishizuka, H., Kamisaka, D., Kurokawa, M., Watanabe, T., Muramatsu, S., Ono, C.: A fundamental study on a indoor localization method using BLE signals and PDR for a smart phone. IEICE Technical report, vol. 114, no. 31, MoNA2014-10, pp. 133–138 (in Japanese)
10. Okabe, A., Boots, B., Sugihara, K., Chiu, S.N.: *Spatial Tessellations: Concepts and Applications of Voronoi Diagrams*, 2nd edn. Wiley, New York (2000)
11. Aurenhammer, F., Schwarzkopf, O.: A simple on-line randomized incremental algorithm for computing higher order Voronoi diagrams. *Int. J. Comput. Geom. Appl.* **2**, 363–381 (1992)
12. Lee, I., Torpelund-Bruin, C., Lee, K.: Map segmentation for geospatial data mining through generalized higher-order Voronoi diagrams with sequential scan algorithms. *Expert Syst. Appl.* **39**(12), 11135–11148 (2012)
13. Halperin, D.: Arrangement. In: Goodman, J.E., O'Rourke, J. (eds.) *Handbook of Discrete and Computational Geometry*, 2nd edn, pp. 529–562. CRC Press, Boca Raton (2004)
14. Apple Inc., iOS: Understanding iBeacon. <http://support.apple.com/kb/HT6048>

Intelligent Software Methodologies, Tools and
Techniques

14th International Conference, SoMet 2015, Naples,
Italy, September 15-17, 2015. Proceedings

Fujita, H.; Guizzi, G. (Eds.)

2015, XVII, 636 p. 276 illus., Softcover

ISBN: 978-3-319-22688-0